Journal of the Indian Institute of Science
A Multidisciplinary Reviews Journal
ISSN: 0970-4140 Coden-JIISAD

REVIEWS

Fermions in Synthetic Non-Abelian Gauge Fields

Sambuddha Sanyal[1], Sudeep Kumar Ghosh[1] and Jayantha P. Vyasanakere[2]

Abstract | Quantum emulation property of the cold atoms has generated a lot of interest in studying systems with synthetic gauge fields. In this article, we describe the physics of two component Fermi gas in the presence of synthetic non-Abelian $SU(2)$ gauge fields. Even for the non-interacting system with the gauge fields, there is an interesting change in the topology of the Fermi surface by tuning only the gauge field strength. When a trapping potential is used in conjunction with the gauge fields, the non-interacting system has the ability to produce novel Hamiltonians and show characteristic change in the density profile of the cloud. Without trap, the gauge fields act as an attractive interaction amplifier and for special kinds of gauge field configurations, there are two-body bound states for any attraction even in three dimensions. For a many body system, the gauge fields can induce a crossover from a weak superfluid to a strong superfluid with transition temperature as high as the Fermi temperature. The superfluid state obtained for a very large gauge field strength is a superfluid of new kind of bosons, called "rashbons", the properties of which are independent of its constituent two component fermions and are solely determined by the gauge field strength. We also discuss the collective excitations over the superfluid ground states and the experimental relevance of the physics.

1 Introduction

In the last decade the subject of synthetic gauge fields in ultra cold atoms received a lot of attention not only in the atomic physics and condensed matter physics community, but also in the high energy physics and field theory community. This recent flurry of activities largely owe to the incredible improvement in cooling and trapping methods of atoms, ions and molecules. The precision in such techniques [1–3] have reached regimes of nano-Kelvin in temperature and angstorm level in position. The realization of Bose Einstein condensation [4] in finite size dilute atomic systems at laboratory, marked the beginning of an era where atomic-molecular physics met condensed matter physics. A major breakthrough in this field came by the possibility of studying exotic many body interacting systems with tunable interactions via Feshbach resonance. Followed by this development the physics of ultra-cold atoms entered the area of strongly correlated systems with the observation of the superfluid-Mott insulator transition in cold atoms in an optical lattice. Since then a large number of efforts were made in emulating quantum systems under a controlled artificial environment.

These realizations of degenerate Bose and Fermi gases in neutral atomic systems at ultra cold temperature where the thermal fluctuations are less than quantum fluctuations, brought us close to Feynman's vision [5] of emulating quantum effects in a controllable set up. In the experimental studies of degenerate Fermi gases in ultra-cold regime an important progress was the observation of long predicted crossover from a weakly attracting Fermi gas in Bardeen-Cooper-Schrieffer (BCS) superfluid state to a Bose Einstein Condensate (BEC) of bosonic molecules, made of strongly attracting fermion pairs. This observation was possible by using Feshbach resonance to tune the interaction between fermions. The next important step was the emulation of systems in the presence of gauge fields in ultra-cold atomic experiments.

[1] *Centre for Condensed Matter Theory, Department of Physics, Indian Institute of Science, Bangalore 560 012, India.*
sambuddha@physics.iisc.ernet.in
sudeep@physics.iisc.ernet.in

[2] *Department of Physics, University College of Science, Tumkur University, Tumkur 572 103, India.*
jayavyasa@gmail.com

The main difficulty in these kind of experiments is that the atoms are charge neutral, thus not affected by external electromagnetic (EM) fields in the way charged particles do. Since the form of the Coriolis force is similar to that of the Lorentz force felt by charge particles in the presence of magnetic fields, there is a possibility of generation of synthetic gauge field by rotating the whole system.[6] But as the procedure suggests, it has inherent technical difficulty and since the strength of the gauge field is proportional to the frequency of rotation, the strength of the gauge field created can not be made very large in which regime most of the interesting physics like the quantum Hall effect occurs. Although this difficulty can be avoided by suitably coupling the hyperfine states of an atom by using Raman transition such that adiabatic evolution of the atom in the ground state manifold mimics a $U(1)$ gauge field.[7,8] This opens up a possibility of emulating fundamental interactions like EM forces which follow from a $U(1)$ gauge field, also weak and strong interactions which are consequences of $SU(2)$ and $SU(3)$ invariant non-abelian gauge fields respectively. However, practical implementation of such dynamical gauge fields as the sources of interaction between elementary particles, remains one of the most challenging prospects for quantum emulations. There are some recent experimental efforts (for bosons[9–12] and for fermions[13,14]) and theoretical proposals[15–20] in experimental realization of synthetic non-Abelian gauge field, but realizing synthetic non-Abelian gauge fields with their full glory is still a dream.

Examples of static gauge fields leading to fascinating physics are many-fold. As mentioned earlier, one can emulate the quantum mechanics of fermions or bosons coupled to EM field by arranging for the neutral particle wave function to pick up the same $U(1)$ phase as that of a charged particle wave function in presence of a real EM field. Similarly, proposals exist for non-Abelian gauge fields by coupling the spin to the orbital motion. Note that unlike the spin orbit interactions encountered in atoms that contribute to spectral fine structure, here the spin is coupled to linear momentum and not angular momentum. The spin orbit term in real materials is found in semiconductor heterostructure, where there is a lack of inversion symmetry in the growth direction, coupling momenta and spins along two directions. Rashba coupling is tuned by varying the gate voltage and is typically weak owing to its origin from a relativistic effect. However, understanding the behavior of such systems is often non-trivial when interactions come into play, also they display exotic physics unparalleled in any other real systems. Since the cold atomic systems allows controlled simulation of gauge fields and spin-orbit coupling, there is a potential to emulate the physics of real solid state systems and help us enriching our understanding of the physics of fractional quantum Hall effect, high T_c etc. Although a uniform Abelian gauge field is merely equivalent to a Galilean transformation, it was shown that even a uniform non-Abelian gauge field gives rise to many interesting physics in case of bosons.[21–25]

In this review we focus on the recent theoretical work[26–30] done mainly by one of the authors of this review (and collaborators) on the behavior of spin -$\frac{1}{2}$ fermions in synthetic non-Abelian $SU(2)$ gauge fields. In section 2, we set up the problem of non interacting fermions in a synthetic non-Abelian $SU(2)$ gauge field, we also discuss the symmetries and scales of the problem. Followed by that we discuss an interesting transition observed in the topology of the Fermi surface, which is driven by the strength of synthetic gauge potential. This section is ended by discussing the prospects of synthesizing novel Hamiltonians by putting this non-interacting system in a trap. Then we turn on a two-body contact interaction between the fermions and discuss its effects in Section 3. The possibility of formation of a novel kind of bound state at arbitrarily weak interaction in three dimension is discussed including the features of that bound state. In the next section we consider interacting many body system with the gauge fields and discuss the possibility of a new kind of BCS-BEC crossover, this BEC is a condensate of a new kind of bound state whose properties depend only on the gauge field. Even in the BCS side we note that the gauge field enhances the transition temperature of this state upto the order of Fermi temperature. This is followed by a discussion of the collective excitations and fluctuations of the superfluid ground state in section 5. The section 6 contains the experimental relevance of the physics discussed in this article and the final section (7) consists of an summary of this article and some possible future directions.

2 Non Interacting Fermions

2.1 *Preliminaries*

Consider a system of non-interacting spin-$\frac{1}{2}$ fermions moving in the continuum of three spatial dimensions in presence of a spatially uniform

and a temporally static $SU(2)$ non-Abelian gauge field. The Hamiltonian of the system is given by:

$$\mathcal{H}_{GF} = \int \mathrm{d}\boldsymbol{r}\, \Psi^\dagger(\boldsymbol{r}) \left[\frac{1}{2}(p_i \mathbf{1} - A_i^\mu \boldsymbol{\tau}^\mu) \times (p_i \mathbf{1} - A_i^\nu \boldsymbol{\tau}^\nu)\right] \Psi(\boldsymbol{r}), \quad (1)$$

where $\Psi(\boldsymbol{r}) = \{\psi_\sigma(\boldsymbol{r})\}, \sigma = \uparrow, \downarrow$ is a two component spinor field (spin quantization along z-axis), p_i is the momentum operator corresponding to i-direction ($i = x, y, z$), $\mathbf{1}$ is the $SU(2)$ identity, $\boldsymbol{\tau}^\mu$ are Pauli spin operators ($\mu = x, y, z$), A_i^μ describe a *uniform* gauge field.

Gauge field configurations of the type $A_i^\mu = \lambda_i \delta_i^\mu$ are of special interest for experiments, of which some have been realized.[10,13,14] A gauge field of that structure, leads to a Hamiltonian of the form,

$$\mathcal{H}_R = \int \mathrm{d}\boldsymbol{r} \Psi^\dagger(\boldsymbol{r}) \left(\frac{\boldsymbol{p}^2}{2}\mathbf{1} - \boldsymbol{p}_\lambda \cdot \boldsymbol{\tau}\right) \Psi(\boldsymbol{r}), \quad (2)$$

with $\boldsymbol{p}_\lambda = \lambda_x p_x \boldsymbol{e}_x + \lambda_y p_y \boldsymbol{e}_y + \lambda_z p_z \boldsymbol{e}_z$. The term containing $\boldsymbol{\tau}^2$ being a constant has no effect on the physics. Thus, the spin orbit coupling of these kind induces a momentum dependent magnetic field on the motion of fermions and the form of the Hamiltonian can be seen as a generalized Rashba type Hamiltonian, with a generic anisotropic spin orbit coupling.

This Rashba gauge field configuration (RGFC) is described entirely by the "vector" $\boldsymbol{\lambda} \equiv \lambda\hat{\boldsymbol{\lambda}} = \lambda_x \boldsymbol{e}_x + \lambda_y \boldsymbol{e}_y + \lambda_z \boldsymbol{e}_z$ where $\lambda = \sqrt{{\lambda_x}^2 + {\lambda_y}^2 + {\lambda_z}^2}$ is the gauge coupling strength. This defines a gauge field configuration (GFC) in the RGFC space as shown in fig. 1(a). In the figure the RGFCs of particular interest are the "extreme oblate" (EO) gauge field with $\boldsymbol{\lambda} = \lambda(\frac{1}{\sqrt{2}}, \frac{1}{\sqrt{2}}, 0)$ which corresponds to the "Rashba spin orbit coupling" encountered in solid state systems[31], the spherical (S) gauge field with $\boldsymbol{\lambda} = \lambda(\frac{1}{\sqrt{3}}, \frac{1}{\sqrt{3}}, \frac{1}{\sqrt{3}})$ and the "extreme prolate" (EP) gauge field with $\boldsymbol{\lambda} = \lambda(0, 0, 1)$.

The symmetry properties of the Hamiltonian in eqn. (2) plays a very important role in the physical behaviors of this system. When $A_i^\mu = 0$, the system possesses three important symmetries, namely: global translational invariance, global phase invariance and time reversal invariance. As A_i^μ is turned on (i.e. $A_i^\mu \neq 0$), translational invariance remains, but the system looses Galilean invariance (this will play a crucial role later), spin rotation and spatial inversion symmetry.

It is also important to note the relevant scales in the problem. The scattering length a_s introduces a length scale while the gauge coupling strength λ introduces a momentum scale. We choose natural units, in which both temperature T and chemical potential μ are of energy dimensions. The finite density ρ of fermions also introduces an energy scale which is the Fermi energy E_F (and an associated Fermi wave vector k_F) in the *absence* of gauge field ($\lambda = 0$) (from now onwards we will sometimes refer this as free vacuum):

$$E_F = \frac{{k_F}^2}{2} = \frac{1}{2}(3\pi^2\rho)^{2/3}. \quad (3)$$

Therefore the dimensionless parameters under consideration are mainly $k_F a_s$, λa_s, λ/k_F, and unit vector $\hat{\boldsymbol{\lambda}}$ in GFC space. In our units $E_F = T_F$.

Now with all these preliminaries being declared, let us look at the non-interacting many fermion system in presence of the synthetic gauge field. The many-body system will be always described in the grand canonical ensemble, where the volume (V), temperature (T) and chemical potential (μ) are held fixed. The term $-\mu\mathcal{N}$ is absorbed into the Hamiltonian, where $\mathcal{N} = \int \mathrm{d}\boldsymbol{r}\, \Psi^\dagger(\boldsymbol{r})\Psi(\boldsymbol{r})$ is the total number operator.

Since the Hamiltonian (eqn. (2)) is translational invariant, momentum $\boldsymbol{k}$ is a good quantum number. However note that spin is no longer a good quantum number due to the presence of "spin-orbit" coupling term. Thus the eigenstates of $\mathcal{H}_R$ in eqn. (2) are given by,

$$|\boldsymbol{k}\alpha\rangle = |\boldsymbol{k}\rangle \otimes |\chi_\alpha(\boldsymbol{k})\rangle \quad (4)$$

where $|\boldsymbol{k}\rangle$ is a plane wave state, $|\chi_\alpha(\boldsymbol{k})\rangle$ is a spin state, $\alpha = \pm 1$ is the generalized helicity. A physical way to think about the helicity quantum number can be following: the Hamiltonian in eqn. (2) produces a "momentum dependent magnetic field"; the positive helicity state ($\alpha = +1$) can be thought of as a spin state $|\chi_+(\boldsymbol{k})\rangle$ that points along this magnetic field, while the negative helicity state $|\chi_-(\boldsymbol{k})\rangle$ is opposite to the magnetic field. Thus one can write down the energy eigenvalues of these states as

$$\varepsilon_\alpha(\boldsymbol{k}) = \frac{\boldsymbol{k}^2}{2} - \alpha|\boldsymbol{k}_\lambda|. \quad (5)$$

As an example, for the S GFC $\varepsilon_\pm(\boldsymbol{k}) = \frac{\boldsymbol{k}^2}{2} \mp \frac{\lambda}{\sqrt{3}}|\boldsymbol{k}|$; for $\boldsymbol{k}$ in the $x-y$ plane this dispersion is plotted in fig. 1(b). For this case, spin state $|\chi_+(\boldsymbol{k})\rangle$ corresponds to a spin in the direction of $\boldsymbol{k}$ and $|\chi_-(\boldsymbol{k})\rangle$ is opposite to $\boldsymbol{k}$.

Next we will consider an interesting effect of Rashba gauge fields on the Fermi surface. As an example we consider the EO gauge field configuration. We noted that for the non-interacting system there are two scales k_F and λ, and the physics

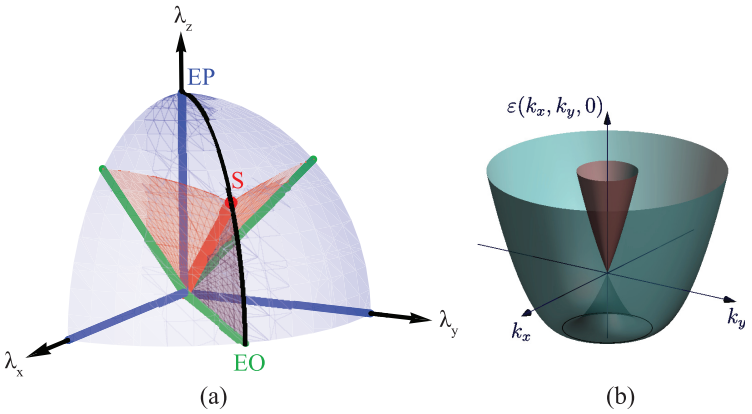

Figure 1: (a) The Rashba gauge field configuration space, where the marked points EP, S and EO represent the extreme prolate, spherical and extreme oblate gauge fields respectively. (b) The energy dispersion of the two helicity eigenstates where the + helicity state (blue) has lower energy than the − helicity state (brown). It is to be noted that the lowest energy has a large number of degenerate states of the + helicity states at the bottom of the + helicity sheet (shown as a blue circle).

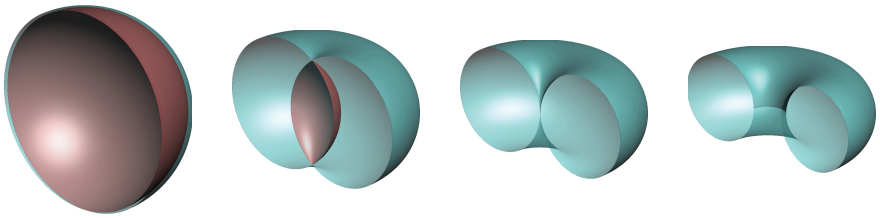

Figure 2: Fermi surface topology transition (FSTT) of noninteracting fermions with increasing the strength λ of the EO gauge field. Half slice of the Fermi surface is shown for different regimes of λ with the + and − helicity Fermi surfaces correspond to dark brown and cyan colors respectively. At $\lambda = \lambda_T$, the Fermi surface associated with the − helicity states vanishes (see (c)), and for $\lambda > \lambda_T$, the states are all of + helicity (shown in (d)).

is governed by the dimensionless parameter λ/k_F, which is the only tunable parameter in this case with the density (ρ) being fixed.

In the absence of the gauge field, the chemical potential μ_{NI} in this non-interacting system is E_F. In presence of the EO gauge field the chemical potential in the regime of small λ is,

$$\frac{(\mu_{NI}(\lambda) - E_F)}{E_F} \sim \left(\frac{\lambda}{k_F}\right)^2 \qquad (\lambda \ll k_F) \tag{6}$$

while for large λ,

$$\frac{(\mu_{NI}(\lambda) - E_F)}{E_F} \sim \frac{k_F}{\lambda} \qquad (\lambda \gg k_F). \tag{7}$$

It is noted that there is a *qualitative* change in the dependence of the chemical potential on λ. This change is manifested also as a change in the topology of the Fermi surface[27] (named as Fermi surface topological transition or FSTT) of the system with increasing λ (as shown in Fig. 2, at $\lambda = \lambda_T$, the Fermi surface associated with the − helicity states vanishes, and for $\lambda > \lambda_T$, the states are all of + helicity. The other highly symmetric gauge fields also show qualitatively similar topological transition in the Fermi surface with increasing strength of the gauge coupling λ.

2.2 *Effect of trapping potential*

The cold atomic experiments are performed in the presence of a trapping potential and information about the properties of the system is obtained by measuring the density profile of the system. In this section, the effects of a spherically symmetric trapping potential on the spin-orbit coupled system are discussed, although the discussions after this section will be in the absence of the trapping potential. Consider an isotropic harmonic trapping potential with frequency ω_0:

$$\mathcal{H}_T = \frac{{\omega_0}^2}{2} \int \mathrm{d}\boldsymbol{r}\, r^2 \psi^\dagger(\boldsymbol{r})\psi(\boldsymbol{r}). \tag{8}$$

This potential spoils the symmetries of the system since it does not commute with the usual kinetic energy term and prevents helicity α to be a good quantum number. Hence, the diagonalization of the full Hamiltonian

$$\mathcal{H} = \mathcal{H}_R + \mathcal{H}_T \tag{9}$$

for a generic ω_0 and $\boldsymbol{\lambda}$ is analytically intractable but identification of important scales in the problem can throw some light into this matter. The single particle Hamiltonian in momentum representation can be written as

$$\mathcal{H}(\boldsymbol{k}) = -\frac{\omega_0^2}{2}\frac{\partial^2}{\partial \boldsymbol{k}^2} + \mathcal{H}_{GF}(\boldsymbol{k}). \tag{10}$$

Although helicity is, in general, no longer an eigenstate of this Hamiltonian, if trap frequency ω_0 is considered to be much smaller compared to the characteristic energy scale associated with the gauge field (such as λ^2 for the Rashba gauge field), one could consider an *adiabatic approximation*, where the helicity is considered as a fast degree of freedom which "instantly equilibrates" with momentum. From this consideration, an adiabatic ansatz can be made for the eigenstates of eqn. (10)

$$|\psi\rangle = \int \mathrm{d}\boldsymbol{k}\, \psi(\boldsymbol{k})\, |\boldsymbol{k}\rangle \otimes |\chi_+(\boldsymbol{k})\rangle \tag{11}$$

using only the $+$ helicity states. The wave function $\psi(\boldsymbol{k})$ is now governed by an effective Hamiltonian of the form

$$H_{\text{eff}} = \frac{\omega_0^2}{2}\left(i\frac{\partial}{\partial \boldsymbol{k}} - \boldsymbol{A}_I\right)^2 + \varepsilon_+(\boldsymbol{k}) + V_{BO}(\boldsymbol{k}) \tag{12}$$

which includes Berry phase effects. The connection $\boldsymbol{A}_I$ is an induced $U(1)$ gauge field given by

$$\boldsymbol{A}_I = -i\left\langle \chi_+(\boldsymbol{k})\middle|\frac{\partial \chi_+(\boldsymbol{k})}{\partial \boldsymbol{k}}\right\rangle \tag{13}$$

and V_{BO} is the Born-Oppenheimer potential

$$V_{BO}(\boldsymbol{k}) = \frac{\omega_0^2}{2}\left(\left\langle \frac{\partial \chi_+(\boldsymbol{k})}{\partial k_i}\middle|\frac{\partial \chi_+(\boldsymbol{k})}{\partial k_i}\right\rangle - \left\langle \frac{\partial \chi_+(\boldsymbol{k})}{\partial k_i}\middle|\chi_+(\boldsymbol{k})\right\rangle\left\langle \chi_+(\boldsymbol{k})\middle|\frac{\partial \chi_+(\boldsymbol{k})}{\partial k_i}\right\rangle\right) \tag{14}$$

(repeated spatial indices i are summed). For the spherical (S) gauge field, the effective Hamiltonian in $\boldsymbol{k}$-space in terms of spherical polar coordinates (k, ϑ, ϕ) has a special form

$$\begin{aligned} H_{\text{eff}} = &-\frac{\omega_0^2}{2}\left(\frac{1}{k^2}\frac{\partial}{\partial k}k^2\frac{\partial}{\partial k}\right) \\ &+ \frac{\omega_0^2}{2k^2}\left[-\frac{1}{\sin\vartheta}\frac{\partial}{\partial\vartheta}\sin\vartheta\frac{\partial}{\partial\vartheta} + \left(\frac{1}{2}\cot\vartheta + \frac{i}{\sin\vartheta}\frac{\partial}{\partial\phi}\right)^2\right] \\ &+ \frac{\omega_0^2}{4k^2} + \left(\frac{k^2}{2} - \frac{\lambda}{\sqrt{3}}k\right). \end{aligned} \tag{15}$$

From this form of the effective Hamiltonian, it is noted that for this gauge field, $\boldsymbol{A}_I$ corresponds to a *monopole* field in momentum space, i.e. this is a realization of a monopole in momentum space (see fig. 3(a))! More interesting phenomena happen for large λ, when the system will be confined to $k \approx \lambda$ due to the Born-Oppenheimer potential. This, then, has a resemblance to the spherical geometry quantum Hall Hamiltonian[32] realized in the momentum representation! The discussion above does not depend upon the statistics of particles and applies to bosons as well.

Hence, when a non-Abelian gauge field is used in conjunction with a trapping potential, there are possibilities of generating interesting quantum Hamiltonians. The trapping potential in conjunction with non-Abelian gauge fields has many other interesting effects on the density profile of the system. The radius of the cloud and the pressure exerted by the system decreases with increasing gauge field strength. These effects lead to characteristic change in the density distribution of the system. For example the spherically symmetric cloud becomes cigar shaped in the presence of EO gauge field (shown in fig. 3(b)).[29]

3 Turning on Interaction

Now we will discuss the effect of turning on the interaction between the fermions in presence of Rashba gauge fields. As discussed in the introduction, one particular advantage in the cold atom systems is that here the interactions are tunable; usually that is done via Feshbach resonance in experiments. The usual Feshbach physics produces a short ranged attraction (in the singlet channel of the fermions), which is described by a scattering length.*

For broad resonances, the scattering length effectively becomes energy independent. In this review we focus on that kind of situations where the fermion interactions are described by an energy-independent scattering length.

*Here the usual custom of quantifying the attraction in terms of the negative inverse of the scattering length is followed.

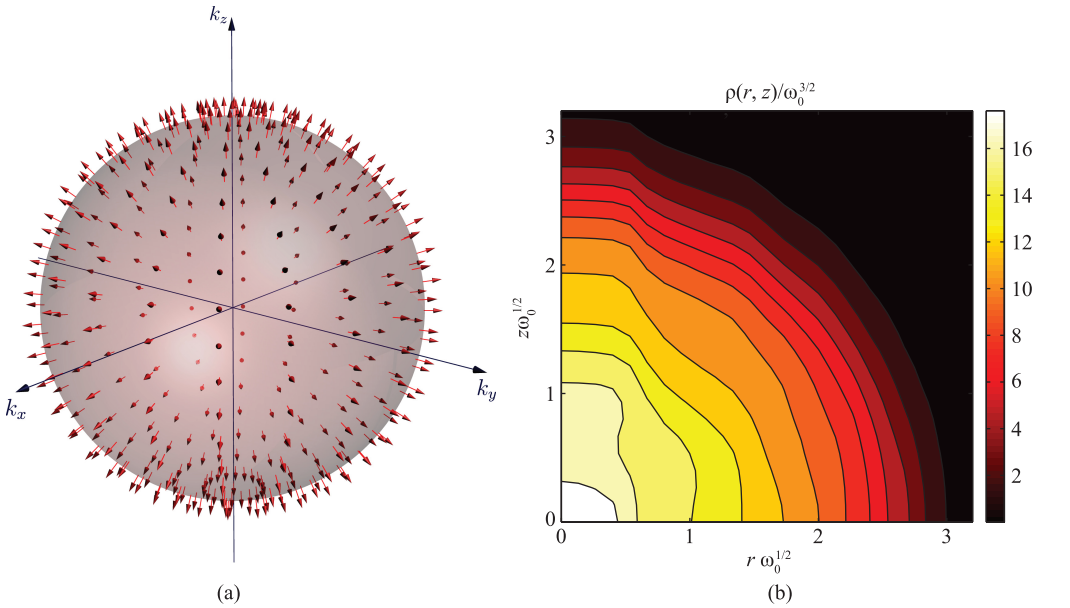

Figure 3: (a) Monopole field induced by an isotropic harmonic potential in conjunction with a Rashba gauge field. For large λ, the particle is confined to move on the sphere $|\boldsymbol{k}| = \lambda$ in momentum space. (b) Contour plot of the spatial density profile of a non-interacting trapped gas in an EO GFC with $\lambda = 20\sqrt{2\omega_0}$. This clearly illustrates the anisotropy in the cloud shape induced by the gauge field. The axes $\boldsymbol{r}$ and z denote in-plane radial coordinate and perpendicular traverse coordinate respectively and the color bar denotes the values of density.

Owing to the extreme dilute nature of cold-atom systems, the particles interact with each other only when they come close enough. Hence the interaction between fermions can be described by a contact attraction model in the singlet channel[33] as

$$\mathcal{H}_\upsilon = \upsilon \int \mathrm{d}\boldsymbol{r}\, \psi_\uparrow^\dagger(\boldsymbol{r})\psi_\downarrow^\dagger(\boldsymbol{r})\psi_\downarrow(\boldsymbol{r})\psi_\uparrow(\boldsymbol{r}), \tag{16}$$

υ is the bare contact interaction. Expressing $\mathcal{H}_\upsilon$ in momentum space, where V is the volume and $C_{\boldsymbol{k}}^\dagger$ is a fermion creation operator in momentum space, the Hamiltonian is given by,

$$\mathcal{H}_\upsilon = \frac{\upsilon}{V} \sum_{\boldsymbol{q}\,\boldsymbol{k}\,\boldsymbol{k}'} C^\dagger_{\frac{\boldsymbol{q}}{2}+\boldsymbol{k}\uparrow} C^\dagger_{\frac{\boldsymbol{q}}{2}-\boldsymbol{k}\downarrow} C_{\frac{\boldsymbol{q}}{2}-\boldsymbol{k}'\downarrow} C_{\frac{\boldsymbol{q}}{2}+\boldsymbol{k}'\uparrow}. \tag{17}$$

Thus contact interaction $\mathcal{H}_\upsilon$ is modeled as a two-body operator that scatters an incoming pair with center of mass momentum $\boldsymbol{q}$ and any relative momentum ($\boldsymbol{k}'$) to the same center of mass momentum and any other relative momentum ($\boldsymbol{k}$) with equal amplitude.

Now the full Hamiltonian that describes our system is given by

$$\mathcal{H} = \mathcal{H}_R + \mathcal{H}_\upsilon. \tag{18}$$

Before the physics of two particles in a non-Abelian gauge field is discussed, let us briefly recall the results[33] of the two body problem in the absence of the gauge field. The theory described by the Hamiltonian in eqn. (18) is ultraviolet divergent and requires a momentum cut-off Λ given by $\Lambda = \frac{1}{V}\sum_{\boldsymbol{k}} \frac{1}{k^2}$. The contact interaction parameter υ is then treated as a flowing coupling constant and is related to the physical scattering length via

$$\frac{1}{\upsilon} + \Lambda = \frac{1}{4\pi a_s}. \tag{19}$$

The point to note and remember is that in free vacuum a critical strength of the attractive interaction is needed to form a bound state of two fermions. In fact, in free vacuum, for $a_s < 0$, there is no bound state. At the resonant scattering length $\frac{1}{a_s} = 0$, the bound state just appears, and exists for $a_s > 0$ with a binding energy of $\frac{1}{a_s^2}$, as is depicted in fig. 4(a). The condition $1/a_s = 0$ is called resonance, where a_s is the s-wave scattering length in the *absence* of the gauge field (see reference[34]).

3.1 *Two-body problem*

The secular equation for the formation of a two-body bound state can be obtained by using a T-matrix analysis which follows very closely the analysis for the two-body problem without gauge fields.[35] The secular equation becomes,

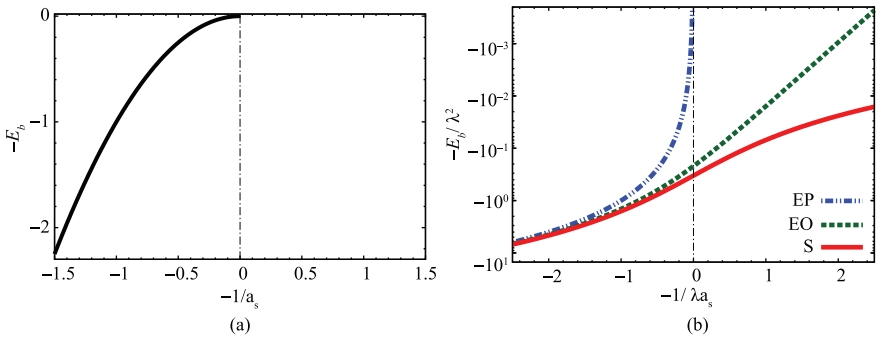

Figure 4: The binding energy of the two body bound state as a function of the scattering length a_s. (a) Shows the case without any gauge field where the vertical line indicates resonant scattering length and (b) shows when there are special kind of gauge field configurations extreme prolate (EP), extreme oblate (EO) and spherical (S). In the EP case, a bound state is obtained only for $1/a_s \geq 0$, while for the other two it is obtained for every a_s. When a_s is small and negative, E_b depends exponentially on λa_s for the EO configurations, while it is a power law in the spherical case.

$$\frac{1}{4\pi a_s} = \frac{1}{V}\sum_{\boldsymbol{k}}\left[\left(\sum_{\alpha\beta}\frac{|A_{\alpha\beta}(\boldsymbol{q},\boldsymbol{k})|^2}{E(\boldsymbol{q})-\varepsilon_{\alpha\beta}(\boldsymbol{q},\boldsymbol{k})}\right)+\frac{1}{k^2}\right]. \tag{20}$$

Here, $A_{\alpha\beta}(\boldsymbol{q},\boldsymbol{k})$ is the singlet amplitude defined as an overlap between the singlet states and two-particle helicity states with relative momentum $\boldsymbol{k}$ and center of mass momentum $\boldsymbol{q}$. E_b is the binding energy defined by $E_b = \varepsilon^s_{th}(\boldsymbol{q}) - E(\boldsymbol{q})$ with $\varepsilon^s_{th}(\boldsymbol{q})$ being the singlet threshold.

Before we go to the discussion on possibilities of bound state formation and nature of the same in specific GFCs, let us discuss the general nature of such a bound state wave function. In free vacuum the bound state wave function is a singlet owing to the fact that spin is a good quantum number with the attraction being in the singlet channel. In contrast, in presence of a non-Abelian gauge field, the normalized bound-state wave function is not a spin eigenstate, thus a superposition of both spatially symmetric singlet and spatially antisymmetric triplet pieces $|\psi_b\rangle = |\psi_s\rangle + |\psi_t\rangle$. A quantity called the triplet content is defined here to measure the weight of the wave function in the triplet sector as

$$\eta_t = \langle\psi_t\psi_t\rangle \tag{21}$$

As we shall see, this quantity plays an important role in both understanding the nature of the two-body bound states and many body ground states.

3.1.1 Results at zero center of mass momentum: We first consider the case when two particles have zero COM momentum ($\boldsymbol{q} = \boldsymbol{0}$). As we turn on the Rashba gauge field,[26] for the EP gauge field (see fig. 1(a)), the condition of bound state formation is identical to that of the free vacuum irrespective of the strength of the gauge coupling λ. A negative scattering length $a_s < 0$, does not allow a bound state, on the other hand a positive scattering length allow formation of bound state with a binding energy $E_b = \frac{1}{a_s^2}$ which is independent of λ.

The EO gauge field shows remarkably different behaviors from EP. In this case the critical scattering length for bound state formation *vanishes*, i.e., no matter what is the scattering length there will be *always* a bound state. The binding energy in the limit of $\lambda|a_s| \ll 1$ and $a_s < 0$ is given by,

$$E_b \approx \frac{2\lambda^2}{e^2} e^{\frac{-2\sqrt{2}}{\lambda|a_s|}}. \tag{22}$$

The S gauge field also displays unique features from EO and EP. Like EO there is a bound state for *any* scattering length, where the binding energy[26] is

$$E_b = \frac{1}{4}\left(\frac{1}{a_s} + \sqrt{\frac{1}{a_s^2}+\frac{4\lambda^2}{3}}\right)^2. \tag{23}$$

For small negative scattering length with $\lambda|a_s| \ll 1$, $E_b \approx (\lambda a_s/3)^2$, indicating much stronger binding even for weak attraction, as depicted in fig. 4(b).

The main difference in presence of high symmetry Rashba gauge fields (along EO-S arc in fig. 1(a)) is the disappearence of critical scattering length a_{sc} necessary for bound state formation. In other words, for these gauge fields, *any* attraction produces a bound state (see fig. 5(b)). The situation is similar for a generic gauge field as shown in

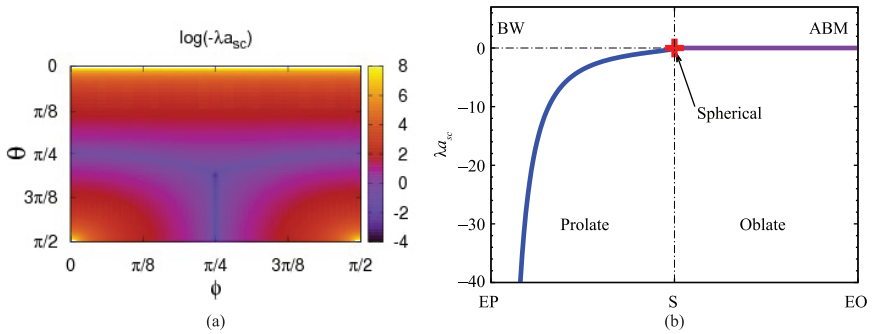

Figure 5: Variation of the critical scattering length a_{sc} for different GFCs. (a) Shows the a_{sc} for a generic GFC as a function of $\hat{\boldsymbol{\lambda}}$ described by θ (polar) and ϕ (azimuthal) angles in GFC space and (b) shows the variation of it along the path EP-S-EO as shown in fig. 1(a). For the EP GFCs, the symmetry of the bound state wave function corresponds to an extended Balian-Werthamer (BW) state with a biaxial nematic spin order, while that in the EO state corresponds to an extended Anderson-Brinkman-Morel (ABM) state with a uniaxial nematic spin order. The state evolves smoothly from a biaxial nematic to a uniaxial nematic passing through the spherical configuration (S) where the bound state is rotationally symmetric.

fig. 5(a), where it is evident that the critical scattering is finite and negative ($a_{sc} < 0$). These result suggest that the Rashba gauge field has the effect of "amplifying" the attractive interaction. For a detailed summary of the two-body bound states in Rashba gauge field look at Table 1.

3.1.2 Rashbon properties-nature of bound state: Next we consider the features of these Rashba bound state wave functions. As noted in the previous section, the total spin of the system is not a conserved quantity in these systems owing to the spin orbit coupling. Further, the interaction in the singlet channel causes mixing between states of different two particle helicity, which causes presence of both singlet and triplet components in orbital part of the bound state wave function. This is characterized by the triplet content η_t (eqn. (21)).

The interesting feature to note here is that the spin structure of the triplet state depends on the gauge field. For the EP gauge field, the triplet state has a spin structure of a bi-axial nematic similar to the BW (Balian-Werthamer) state of ^{3}He, while for the EO gauge field the spin structure is a uniaxial spin nematic like that of the ABM (Anderson-Brinkman-Morel) state of ^{3}He.[36] Indeed, the spin structure of the triplet piece evolves smoothly (see fig. 5(a)) from the biaxial nematic to a uniaxial nematic in going along the EP-S-EO arc in fig. 1(a). It is emphasized that this spin structure does not owe to a spontaneously broken symmetry (as in ^{3}He), but is more like the spin structure obtained in spin-orbit coupled unconventional superconductors[37] where the spin structure of the pair is imposed by the symmetry of the spin-orbit interaction.

The main point to note here is the two body bound state obtained in a Rashba gauge field with a resonant scattering length, as we will see later the properties of such a bound state is solely dependent on the Rashba gauge field. Hence, such bound state of two fermions at resonant scattering length is called the *rashbon*.[27] For a detailed summary of the two-body bound states in Rashba gauge field look at Table 1.

Now let us look at the properties of Rashbon bound state in high symmetry gauge fields such as those along the EO-S-EP arc in fig. 1.[28] These gauge fields are conveniently described by $\boldsymbol{\lambda} = (\lambda_l, \lambda_l, \lambda_r)$; we also use $\sin\theta = \lambda_r/\lambda$ in the discussions. For such a gauge field the rashbon mass is anisotropic with an "in-plane" mass m_l^R and "perpendicular" mass m_r^R defined as

$$\frac{1}{m_l^R} = \left.\frac{\partial^2 E_R(q_l, q_r)}{\partial q_l^2}\right|_{\boldsymbol{q}=\boldsymbol{0}}, \qquad \frac{1}{m_r^R} = \left.\frac{\partial^2 E_R(q_l, q_r)}{\partial q_r^2}\right|_{\boldsymbol{q}=\boldsymbol{0}} \tag{24}$$

where $\boldsymbol{q} = (q_l, q_l, q_r)$. The effective mass

$$m_{\rm ef}^R = \sqrt[3]{m_r^R m_l^2}. \tag{25}$$

The dispersion $E(\boldsymbol{q})$ calculated by solving eqn. (20) is in general anisotropic setting. However, due to their symmetry, for the GFCs considered in this section, $E_R(\boldsymbol{q}) = E(q_l, q_r)$, where q_l is the component of $\boldsymbol{q}$ on the $x-y$ plane, and q_r is the component along $\boldsymbol{e}_z$.

Fig. 6 shows a plot of the mass and the triplet content of rashbons. What is noteworthy is that the rashbon mass, while larger than 2 (twice fermion

Table 1: The binding energy E_b, the triplet content η_t and spin structure obtained from the analysis of the two-body problem for special GFCs are summarized here. The values of E_b and η_t at resonance are exact results, while others are asymptotic values.

GFC	a_{sc}	$a_s<0$, $\lambda\lvert a_s\rvert \ll 1$			Resonance, $1/(\lambda a_s)=0$			$a_s>0$, $\lambda a_s \ll 1$		
		E_b	η_t	Spin Structure	E_b	η_t	Spin Structure	E_b	η_t	Spin Structure
EP	$-\infty$	No bound state			0	$\frac{1}{2}$	Bi-axial nematic (BW)	$\frac{1}{{a_s}^2}$	0	singlet
S	0^-	$\frac{\lambda^4 {a_s}^2}{3}$	$\frac{1}{2}$	Spherical	$\frac{\lambda^2}{3}$	$\frac{1}{4}$	Spherical	$\frac{1}{{a_s}^2}+\frac{2\lambda^2}{3}$	0	singlet
EO	0^-	$\frac{2}{e^2}e^{-\frac{2\sqrt{2}}{\lambda\lvert a_s\rvert}}$	$\frac{1}{2}$	Uni-axial nematic (ABM)	$0.22\lambda^2$	0.28	Uni-axial nematic (ABM)	$\frac{1}{{a_s}^2}+\frac{\lambda^2}{2}$	0	singlet

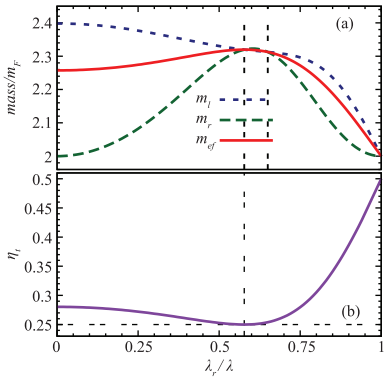

Figure 6: Properties of rashbons as a function of $\boldsymbol{\lambda} = (\lambda_l, \lambda_l, \lambda_r)$ for different GFCs along the arc shown in fig. 1(a). Here (a) shows in-plane, perpendicular and effective masses and (b) shows the triplet content (eqn. (21)) of the rashbons.

mass), is never very much greater than 2. In fact the largest effective mass occurs for the S gauge field for which $m^R = m^R_{\rm ef} = \frac{3}{7}(4+\sqrt{2}) \approx 2.32$. We will see in next section that this "lightness" of the rashbons will be responsible for enhancing the transition temperature of superfluid ground states.

3.1.3 Results at finite center of mass momentum: In this section we will discuss the effects of Rashba gauge field on the fermionic system with two body interactions at a non zero value of COM momentum $\boldsymbol{q}$. Let us first briefly recall the known results in free vacuum. In the absence of the gauge field, the threshold energy $\varepsilon_{th}(\boldsymbol{q}) = \frac{q^2}{4}$. For a negative scattering length, there is no bound state, while for a positive scattering length $E(\boldsymbol{q}) = \frac{q^2}{4} + \frac{1}{a_s^2}$.

Now let us turn on the highly symmetric S gauge field and first look at the "dispersion" relation for the bound state,[28] i.e., the function $E_R(\boldsymbol{q})$ in fig. 7(a). First note that the scattering threshold is *independent* of $q = |\boldsymbol{q}|$ in the regime $q \le q_0 = \frac{2}{\sqrt{3}}\lambda$. In that regime, the bound state energy $E_R(q)$ increases for all scattering lengths, which means that the binding energy decreases with increasing q. On the other hand we know that if we turn off the Rashba gauge field the binding energy is independent of q. The most important new feature here is that for a given scattering length there is a critical COM momentum above which there is *no bound state* (shown in fig. 7(b)).

When $q < q_0$, the critical scattering length required for bound state formation vanishes, i.e., there is a bound state for any scattering length. As we just mentioned, for $q > q_0$, the critical scattering length required to form a bound state is not zero. For very large COM momenta $q \gg \lambda$, a *small positive* critical scattering length $a_{sc} \sim \frac{1}{\sqrt{q}}$ is necessary to produce a bound state. In other words, at large COM momenta, the same attractive interaction which produces a bound state in free vacuum is unable to produce a bound state in the presence of the gauge field. The gauge field which acted to *promote* bound state formation at small COM momenta, acts in exactly opposite manner at large COM momenta in that it *inhibits* bound state formation at large COM momenta.

The physics behind all these can be understood from the behavior of infrared singlet density of states. At zero COM the non-Abelian gauge fields act to enhance the infrared singlet density of states. This enables the particles to form bound states easily. The same situation prevails for $q \le q_0$. However, at $q = q_0$ there is a qualitative

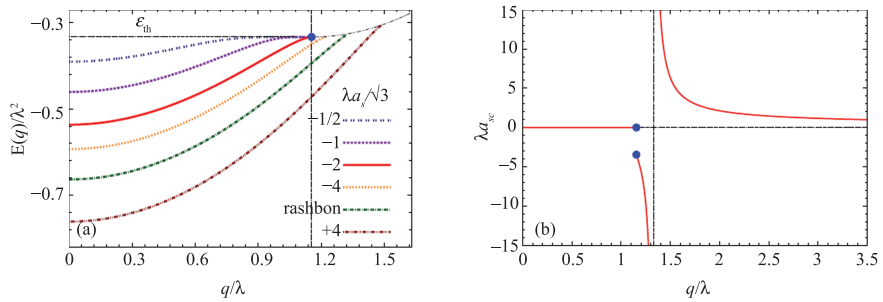

Figure 7: (a) Dispersion of the two body bound states as a function of center of mass momentum for various scattering lengths in spherical GFC. It is noted that for any given scattering length, the bound state disappears after a critical momentum. (b) Critical scattering length (a_{sc}) as a function of center of mass momentum. This critical scattering length a_{sc} goes as $1/\sqrt{q}$ in the large q/λ limit.

change, caused by the gauge field, in the nature of the low energy singlet density of states.[28] This is also reflected in the jump of critical scattering length (see fig. 7(b)). The gauge field depletes the population of low energy singlet states, which is responsible for the inhibition of the bound state formation at large COM.

3.2 *Many body problem*

In this section we will consider the effect of interaction on many-body system of fermions in a Rashba gauge field. Like before. Let us recall before we turn on the gauge field, the ground state of the finite density of fermions in presence of a contact singlet attraction (eqn. (16)) is a superfluid state[36,38] for any scattering length a_s. Here we will[27] follow the evolution of the system starting from this superfluid state with an increasing value of the strength of the gauge coupling (Rashba spin-orbit interaction-λ (for a given $\hat{\boldsymbol{\lambda}}$). In this section we will discuss the ground states of the many body system within the scope of a mean field picture. The mean field ansatz involves providing an static expectation value of the operator $S^\dagger(\boldsymbol{q})$ defined in eqn. (27).

The full Hamiltonian eqn. (18) of the system can be rewritten as

$$\mathcal{H} = \sum_{\boldsymbol{k}\alpha} \xi_{\boldsymbol{k}\alpha} C^\dagger_{\boldsymbol{k}\alpha} C_{\boldsymbol{k}\alpha} + \frac{\upsilon}{2V} \sum_{\boldsymbol{q}} S^\dagger(\boldsymbol{q}) S(\boldsymbol{q}) \quad (26)$$

where, $\xi_\alpha(\boldsymbol{k}) = \varepsilon_\alpha(\boldsymbol{k}) - \mu$. The operator $S^\dagger(\boldsymbol{q})$ creates a singlet with center of mass momentum $\boldsymbol{q}$ and is defined as

$$S^\dagger(\boldsymbol{q}) = \sum_{\boldsymbol{k}} \underbrace{\frac{1}{\sqrt{2}} \left(C^\dagger_{\frac{\boldsymbol{q}}{2}+\boldsymbol{k},\uparrow} C^\dagger_{\frac{\boldsymbol{q}}{2}-\boldsymbol{k},\downarrow} - C^\dagger_{\frac{\boldsymbol{q}}{2}+\boldsymbol{k},\downarrow} C^\dagger_{\frac{\boldsymbol{q}}{2}-\boldsymbol{k},\uparrow} \right)}_{S^\dagger(\boldsymbol{q},\boldsymbol{k})}. \quad (27)$$

The non-interacting Hamiltonian is quadratic in fermion operators and hence was diagonalized analytically. But the interaction term being quartic, we perform a mean field approximation. The mean field form of the full Hamiltonian turns out to be

$$\begin{aligned} \mathcal{H}_{MF} = & \sum_{\boldsymbol{k}\alpha}{}' \begin{pmatrix} C^\dagger_{\boldsymbol{k}\alpha} & C_{-\boldsymbol{k}\alpha} \end{pmatrix} \\ & \times \begin{bmatrix} \xi_{\boldsymbol{k}\alpha} & \alpha\Delta_0 \\ \alpha\Delta_0 & -\xi_{\boldsymbol{k}\alpha} \end{bmatrix} \begin{pmatrix} C_{\boldsymbol{k}\alpha} \\ C^\dagger_{-\boldsymbol{k}\alpha} \end{pmatrix} \\ & + \sum_{\boldsymbol{k}\alpha}{}' \xi_{\boldsymbol{k}\alpha} - \frac{V{\Delta_0}^2}{\upsilon} \end{aligned} \quad (28)$$

where, $\sum'$ denotes the sum over only half of the k-space, $\Delta_0 = \frac{\upsilon\langle S^\dagger(\boldsymbol{0})\rangle}{\sqrt{2}V}$ is the excitation gap (also called pairing amplitude or order parameter) which, without loss of generality, is taken as real.

Defining Bogoliubov operators $\gamma_{\boldsymbol{k}\alpha 1} = (u_{\boldsymbol{k}\alpha} C_{\boldsymbol{k}\alpha} - \alpha v_{\boldsymbol{k}\alpha} C^\dagger_{-\boldsymbol{k}\alpha})$ and $\gamma^\dagger_{\boldsymbol{k}\alpha 2} = (\alpha v_{\boldsymbol{k}\alpha} C_{\boldsymbol{k}\alpha} + u_{\boldsymbol{k}\alpha} C^\dagger_{-\boldsymbol{k}\alpha})$ with $u^2_{\boldsymbol{k}\alpha} = \frac{1}{2}\left(1 + \frac{\xi_{\boldsymbol{k}\alpha}}{E_{\boldsymbol{k}\alpha}}\right), v^2_{\boldsymbol{k}\alpha} = \frac{1}{2}\left(1 - \frac{\xi_{\boldsymbol{k}\alpha}}{E_{\boldsymbol{k}\alpha}}\right)$ and $E_{\boldsymbol{k}\alpha} = \sqrt{\xi^2_{\boldsymbol{k}\alpha} + {\Delta_0}^2}$, the diagonalised mean field Hamiltonian takes the form

$$\begin{aligned} \mathcal{H}_{MF} = & \sum_{\boldsymbol{k}\alpha}{}' E_{\boldsymbol{k}\alpha} \left(\gamma^\dagger_{\boldsymbol{k}\alpha 1} \gamma_{\boldsymbol{k}\alpha 1} + \gamma^\dagger_{\boldsymbol{k}\alpha 2} \gamma_{\boldsymbol{k}\alpha 2} \right) \\ & + \sum_{\boldsymbol{k}\alpha}{}' (\xi_{\boldsymbol{k}\alpha} - E_{\boldsymbol{k}\alpha}) - \frac{V{\Delta_0}^2}{\upsilon}. \end{aligned} \quad (29)$$

It may appear that for each helicity there are two branches of quasi-particle excitations labeled 1 and 2, making the total count four. However, these four branches are defined only in half of the momentum space. If the Bogoliubov excitations were defined for all $\boldsymbol{k}$, they will not be independent, for example, $\gamma^\dagger_{\boldsymbol{k}+2} \equiv \gamma^\dagger_{-\boldsymbol{k}+1}$. This is the reason for performing the sum over only half of the momentum space. Hence, this formulation recovers the correct count of excitations.

At a temperature T, we obtain the thermodynamic potential $\mathcal{F}$ as

$$V\mathcal{F}(T,\mu,\Delta) = -T\sum_{\boldsymbol{k}n}{}' \ln\left(1+e^{-\frac{E_n(\boldsymbol{q},\boldsymbol{k})}{T}}\right) + \sum_{\boldsymbol{k}\alpha}{}' \xi_\alpha\left(\frac{\boldsymbol{q}}{2}-\boldsymbol{k}\right) - \frac{V\Delta^2}{\upsilon} \quad (30)$$

where $E_n(\boldsymbol{q},\boldsymbol{k})$ with n =1,4, are the eigenvalues of the mean field Hamiltonian written in the helicity basis. The equilibrium values of Δ and μ are determined by minimizing the free energy and hence

$$\frac{\partial\mathcal{F}}{\partial\Delta} = 0, \quad (31)$$

and the number equation

$$-\frac{\partial\mathcal{F}}{\partial\mu} = \rho. \quad (32)$$

These lead to the gap equation

$$\frac{1}{4\pi a_s} = \frac{1}{2V}\sum_{\boldsymbol{k}\,\alpha}\left(-\left(\frac{1-2\,n_F\left(E_{\boldsymbol{k}\alpha}\right)}{2E_{\boldsymbol{k}\alpha}}\right)+\frac{1}{k^2}\right) \quad (33)$$

and the number equation

$$\rho = \frac{1}{V}\sum_{\boldsymbol{k}\,\alpha}\frac{1}{2}\left(1-\frac{\xi_{\boldsymbol{k}\alpha}}{E_{\boldsymbol{k}\alpha}}\left(1-2n_F\left(E_{\boldsymbol{k}\alpha}\right)\right)\right). \quad (34)$$

The simultaneous solution of eqn. (33) and eqn. (34) determines the chemical potential μ and the gap parameter Δ_0 at that temperature.

The ground state of the system is given by

$$|\Psi_G\rangle = \prod_{\boldsymbol{k}\alpha}{}'(u_{\boldsymbol{k}\alpha}+\alpha v_{\boldsymbol{k}\alpha}C^\dagger_{\boldsymbol{k}\alpha}C^\dagger_{-\boldsymbol{k}\alpha})|0\rangle \quad (35)$$

where $|0\rangle$ is the fermion vacuum. The triplet content η_t for the many-body ground state is defined as the weight of the triplet sector of the pair creation operator. We will see in this section that in the presence of an attractive interaction in the singlet channel, the pairs have a triplet content less than that of the noninteracting system.

3.2.1 BCS-BEC crossover induced by the gauge field: We will now follow the nature of the many body ground state by gradually increasing the gauge field strength starting from zero. First let us recall that in free vacuum the many body superfluid state goes through a BCS-BEC crossover which is induced by tuning the attraction (scattering length a_s).

Now as we turn on the Rashba gauge field, the most interesting effect occurs at small negative scattering lengths. For small λ, i.e., $\lambda \ll \lambda_T$, the system is described by the BCS theory, the excitation gap- Δ_0 is exponentially small and the chemical potential is same as that of the noninteracting problem for S GFC. Except for the less symmetric EP GFC, when λ is increased beyond λ_T, the chemical potential μ begins to fall and approaches $-E_b/2$, i.e. energy of the two-body bound state. Additionally, the pair wave function can be seen to approach the two-body bound state wave function. This signals the onset to the BEC state. Notice the important difference here, this BCS-BEC crossover is by the gauge field at a fixed attraction whereas the one in free vacuum is induced by attraction.

On the other hand for small positive scattering lengths, the system is already a BEC even in free vacuum. The pair wave function is a singlet, i.e., $\eta_t = 0$. By tuning λ, the system continues to be a BEC, but picks up a triplet component.

For details of this crossover we again choose the case for S-GFC as a representative case, for which Fig. 8(a) and (b) show, respectively, the numerical solutions of the chemical potential and gap as a function of λ. Fig. 8(a) also shows the noninteracting chemical potential, and the two-body energy $-E_b/2$ (which depends on λ and a_s only). As is evident the chemical potential μ is same as the noninteracting value $\mu_{NI}(\lambda)$ for $\lambda \ll \lambda_T$. When $\lambda \to \lambda_T$ the chemical potential begins to fall below μ_{NI}, and on further increase of λ ($\lambda \gtrsim \lambda_T$), the chemical potential tends towards that of the two-body problem. This is a clear sign of a crossover from the BCS like state for $\lambda \ll \lambda_T$ to a BEC state at the zero center of mass momentum.

More evidence to the crossover to the BEC like state with increasing λ can be obtained by a study of the triplet content η_t which is shown in fig. 8(c). η_t of the noninteracting system monotonically increases and attains a value of $\frac{1}{2}$ at λ_T. The triplet content of the superfluid pair, as expected, is less than that of the noninteracting system, but has a similar qualitative behavior as the NI case in the regime $\lambda \ll \lambda_T$. The triplet content attains a maximum at a λ close to λ_T and then begins to fall. On further increase of λ, η_t approaches that of the *two-body* bound-state wave function, demonstrating again that the pair wave function tends to the two-body bound-state wave function. We also see that $\lambda = \lambda_T$ marks the crossover regime, that is precisely the regime of λ where change in the topology of the noninteracting Fermi sea takes place.

We note that the qualitative nature of the results for negative scattering lengths ($a_s < 0$) of larger

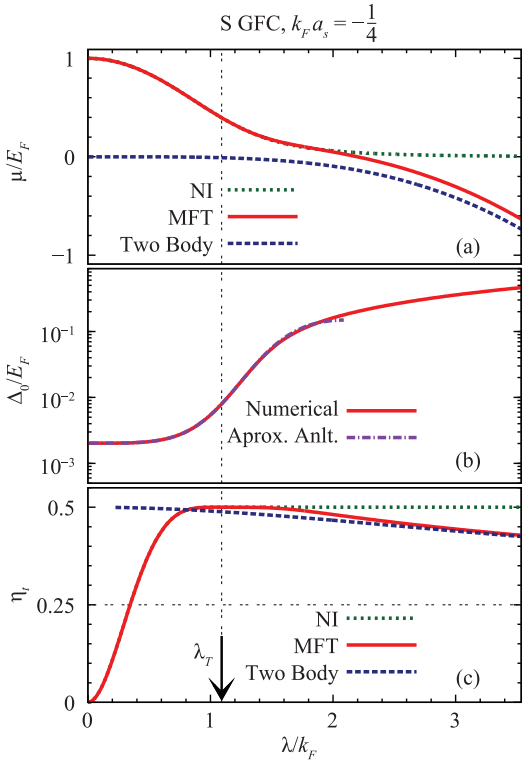

Figure 8: Evolution of the ground state of a collection of interacting fermions ($k_F a_s = -\frac{1}{4}$) with gauge-coupling strength λ for the S GFC. (a) Chemical potential obtained from a numerical solution of mean field theory (MFT) is compared with that of the noninteracting system (NI) and that set by the binding energy of the two-body problem ($-E_b/2$). (b) Dependence of the numerically obtained excitation gap Δ_0 with the gauge-coupling strength λ and its approximate analytic form for $\lambda \ll \lambda_T$ are shown. (c) The dependence of the triplet content (η_t) of the pair wave function λ. This is compared with that of the noninteracting system (NI) and with that of the wave function of the two-body bound state.

magnitude are similar to those for $k_F|a_s| \ll 1$. We summarize the BCS-BEC crossover properties for various GFCs in Table 2.

In this context it will be interesting to note the evolution of dispersion of the Bogoliubov quasiparticles as a function of gauge coupling strength λ with particular focus on negative scattering lengths. The gauge-coupling strength at which the chemical potential $\mu(\lambda)$ equals that of the noninteracting system at the FSTT is defined as λ_B. Note that λ_B, in general, depends on the scattering length a_s with $\lambda_B \approx \lambda_T$ when $k_F|a_s| \ll 1$. It turns out that as $\lambda < \lambda_B$, there exists low lying quasi particle excitations of both helicity. At the transition point $\lambda = \lambda_B$, the low lying $-$ helicity excitation appears at $\boldsymbol{k} = 0$, and for $\lambda > \lambda_B$, there are no low-lying excitations corresponding to $-$ helicity. The transition in the topology of the dispersion of the Bogoliubov quasiparticles at λ_B can be owed to the FSTT as for $k_F|a_s| \ll 1$, this transition in the quasi particle spectrum very nearly coincides with FSTT.

3.2.2 Properties of Rashbon BEC: As discussed earlier in this section, for $\lambda \to \infty$, the BEC is formed by a new kind of particles. It is interesting to explore the properties of this BEC state. The special feature in the presence of the gauge field is that the physics of the two-body bound state is fully determined by the dimensionless parameter λa_s. Hence, the obtained state is same as that obtained for the two-body bound state with a resonant scattering length in the presence of the gauge field ($\lambda > 0$). This bound bosonic pairs constituted of two fermions are named to be "rashbon". Hence, the properties of the BEC for $\lambda \to \infty$ are completely determined by $\boldsymbol{\lambda}$ and is independent of the scattering length (as long as it is nonzero), i.e., *the system is a collection of bosons whose properties are determined solely by the Rashba gauge field* which is named to be RBEC (rashbon Bose Einstein condensate).

We now discuss, the limit of large λ for an arbitrary GFC in more detail. In RBEC ($\lambda \gg k_F, \frac{1}{a_s}$), it is noted that $\mu < 0$ and $|\mu| \simeq \frac{E_b}{2} \simeq \frac{\lambda^2}{2}\mathcal{R}(\hat{\boldsymbol{\lambda}}) \gg \Delta_0$, where $\mathcal{R}(\hat{\boldsymbol{\lambda}})$ is a dimensionless function of the gauge field configuration. In this regime, $E_{\boldsymbol{k}\alpha} \simeq \xi_{\boldsymbol{k}\alpha}$, and the number equation (eqn. (34)) for zero temperature becomes

$$\rho \simeq \frac{{\Delta_0}^2}{2V}\sum_{\boldsymbol{k}\alpha}\frac{1}{2\left(\tilde{\varepsilon}_\alpha(\boldsymbol{k}) + \frac{\lambda^2}{2}\mathcal{R}(\hat{\boldsymbol{\lambda}})\right)^2}, \tag{36}$$

where $\tilde{\varepsilon}_\alpha(\boldsymbol{k}) = \varepsilon_\alpha(\boldsymbol{k}) + \frac{{\lambda_{\max}}^2}{2}$ and $\lambda_{max} = \text{Maximum}(\lambda_x, \lambda_y, \lambda_z)$. The above equation can be rewritten as

$${\Delta_0}^2 = \rho\,\lambda\,H(\hat{\boldsymbol{\lambda}}), \tag{37}$$

where $H(\hat{\boldsymbol{\lambda}})$ is a dimensionless number which depends only on the GFC.

The regularized gap equation (eqn. (33)) at zero temperature takes the form

$$-\frac{1}{4\pi a_s^{ef}} = B(2|\mu|, \boldsymbol{\lambda}), \tag{38}$$

Table 2: Summary of the properties of the superfluid ground state for two regimes of the gauge-coupling strength λ. The results shown here are for a weak attractive interaction ($a_s < 0$; $k_F|a_s| \ll 1$). μ is the ground state chemical potential and η_t is the triplet content of the pair wave function. Well before the FSTT ($\lambda \ll \lambda_T$), the ground state is a BCS superfluid. In the regime ($\lambda \gg \lambda_T$), for the S and EO GFCs, the chemical potential is close to half of the rashbon energy (see Table. I) and the pair wave function attains the same triplet content as that of the rashbon, clearly indicating a crossover from a BCS superfluid to a rashbon condensate. Any GFC *except* EP produces a BCS—rashbon BEC crossover.

GFC	λ_T	$\lambda \ll \lambda_T$ Before FSTT		$\lambda \gg \lambda_T$ After FSTT		Crossover to rashbon-BEC
		μ	η_t	μ	η_t	as $\lambda \to \infty$?
EP	k_F	$\approx E_F$	$\propto \lambda^2$	$\approx E_F$	$\frac{1}{2}$	No
S	$\frac{\sqrt{3}}{2^{(2/3)}} k_F$	$\approx \mu_{NI}(\lambda)$	$\propto \lambda^2$	$\approx -\frac{\lambda^2}{6}$	$\approx \frac{1}{4}$	Yes
EO	$\left(\frac{8\sqrt{2}}{3\pi}\right)^{\frac{1}{3}} k_F$	$\approx \mu_{NI}(\lambda)$	$\propto \lambda^2$	$\approx -0.11\lambda^2$	≈ 0.28	Yes

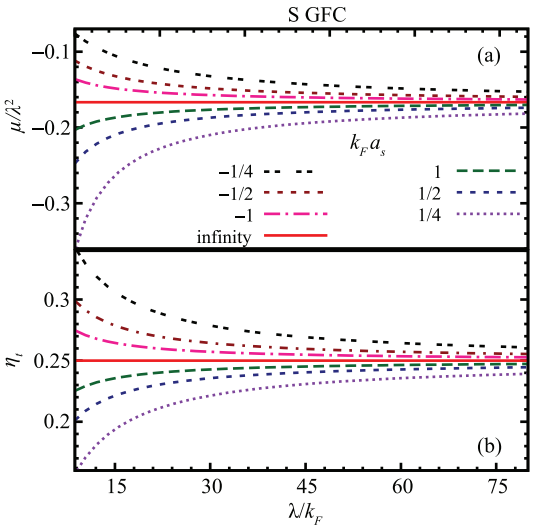

Figure 9: Dependence of chemical potential (μ) and triplet content (η_t) on gauge-coupling strength λ (S GFC) in the $\lambda \gg \lambda_T$ regime, for various scattering lengths a_s. (a) Chemical potential, for all scattering lengths, asymptotically attains the value set by the rashbon energy (see Table 1) as $\lambda/k_F \to \infty$. (b) Triplet content also attains the rashbon value independent of the scattering length.

where,

$$B(E_b, \boldsymbol{\lambda}) = \frac{1}{2V}\sum_{\boldsymbol{k}\alpha}\left(\frac{1}{2\tilde{\varepsilon}_\alpha(\boldsymbol{k}) + E_b} - \frac{1}{k^2}\right),$$

$$\frac{1}{a_s^{ef}} = \frac{1}{a_s} - 4\pi{\Delta_0}^2\frac{G(\hat{\boldsymbol{\lambda}})}{\lambda^3}.$$

Here, $G(\hat{\boldsymbol{\lambda}})$ is another dimensionless number that depends only on the GFC. Solving the above equation, the chemical potential can be approximated as

$$\mu = -\frac{\lambda^2\mathcal{R}(\hat{\boldsymbol{\lambda}})}{2} + \frac{1}{2}M(\hat{\boldsymbol{\lambda}})\frac{\rho}{\lambda}, \tag{39}$$

where, $M(\hat{\boldsymbol{\lambda}}) = 2H(\hat{\boldsymbol{\lambda}})^2\, G(\hat{\boldsymbol{\lambda}})$.

The dimensionless function $M(\hat{\boldsymbol{\lambda}})$ is shown in fig. 10 for important set of GFCs. For spherical (S) GFC, these quantities evaluate to $H = \frac{2\pi}{\sqrt{3}}$, $G = \frac{3\sqrt{3}}{4\pi}$ and $M = 2\pi\sqrt{3}$. The quantity $M(\hat{\boldsymbol{\lambda}})$ is very important since the effective rashbon-rashbon scattering length and properties of the superfluid depends on it.

4 Estimation of Transition Temperature

Two different procedures of estimation of the transition temperature are first outlined. On the BCS

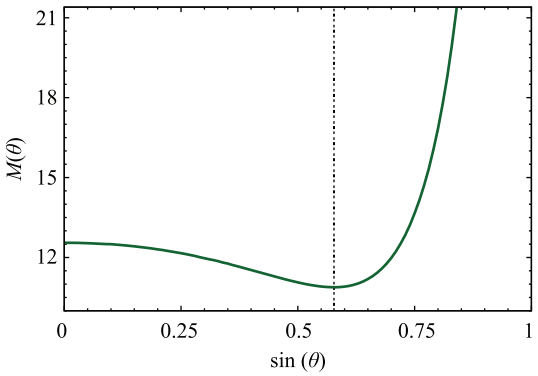

Figure 10: The effective rashbon chemical potential $\mu_R = M(\hat{\boldsymbol{\lambda}})\frac{\rho}{\lambda}$ and the effective rashbon-rashbon scattering length $a_R = \frac{M(\hat{\boldsymbol{\lambda}})m_R^{ef}}{2\pi\lambda}$ with m_R^{ef} being the effective rashbon mass. The plot shows $M(\hat{\boldsymbol{\lambda}})$ for high symmetry Rashba gauge fields such as those along the arc EO-S-EP shown in fig. 1(a) where $\hat{\boldsymbol{\lambda}} = \left(\frac{\cos\theta}{\sqrt{2}}, \frac{\cos\theta}{\sqrt{2}}, \sin\theta\right)$ where $\sin\theta = \frac{\lambda_r}{\lambda}$.

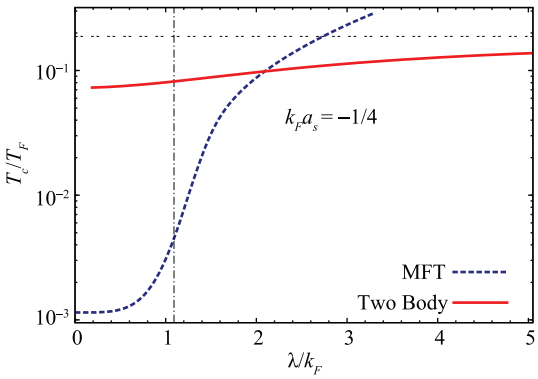

Figure 11: Transition temperature T_c estimate for the S GFC as a function of λ. T_c in small and large λ/k_F limits are obtained from mean field theory and condensation temperature of two body bound pairs respectively. Horizontal and vertical dashed lines correspond to rashbon T_c and $\lambda = \lambda_T$ respectively.

side the transition from a superfluid state to a normal state is indicated by vanishing of the gap Δ_0. So one can estimate the transition temperature (T_c) from the mean field equations of gap (eqn. (33)) and number density (eqn. (34)) by simultaneously solving for T and μ. On the other hand, in case of the transition from BEC regime, pair breaking becomes energetically costly. In this case T_c is governed by phase fluctuations and can be estimated as the Bose condensation temperature of the tightly bound (anisotropic) bosonic pairs of fermions. This is given by,

$$\frac{T_c}{T_F} = \left(\frac{16}{9\pi(\zeta(3/2))^2}\right)^{1/3}\frac{1}{m_{ef}}, \tag{40}$$

where m_{ef} is the effective mass of the bosons determined by the low energy dispersion as a function of $\boldsymbol{q}$.

How these considerations apply to free vacuum and how much do they agree with the fluctuation calculation in their respective regimes will be discussed in section 5. These calculations are extended to include different GFCs (T_c in EO GFCs was also calculated in reference[39] to which these results agree). In fig. 11 we show that at a fixed small negative a_s for $\lambda \ll k_F$ the transition temperature T_c of the BCS like superfluid is determined by the mean field theory and hence is exponentially small. However, for the regime of large λ, the system is like a RBEC, T_c is determined by eqn. (40) and is of the order of Fermi temperature T_F! These findings are quite remarkable. In other words, *an exponentially small T_c of a weak superfluid can be enhanced to the order of Fermi temperature by tuning only the Rashba gauge field strength without having to increase the interaction.*

When a_s is a small positive number, the T_c for all values of λ is given by eqn. (40). Whatever be the scattering length, when $\lambda \to \infty$, the T_c tends to that determined by the rashbons and depends only on $\hat{\boldsymbol{\lambda}}$ through the effective mass m_{ef}. m_{ef} for important GFCs is shown in fig. 6(a). Since effective rashbon mass for S GFC is largest, it has the smallest rashbon T_c ($\approx 0.188T_F$).

5 Collective Excitations

The collective excitations of a superfluid has many interesting properties and study of these is naturally motivated by questions like those regarding the stability of the superfluid. A functional integral framework, which has been used extensively in the context of BCS-BEC crossover, is used.[30] A general framework is formulated for arbitrary temperature T although the primary interest is to study zero temperature properties. The action of the system can be written as

$$\mathcal{S}[c] = \sum_{k,k'} c^\star(k)_\sigma(-G^{-1}_{0\sigma,\sigma'}(k,k'))c_{\sigma'}(k') + \frac{Tv}{V}\sum_q S^\star(q)S(q), \tag{41}$$

where cs and $c^\star$s are Grassmann fields corresponding to the fermions and the free (without interac-

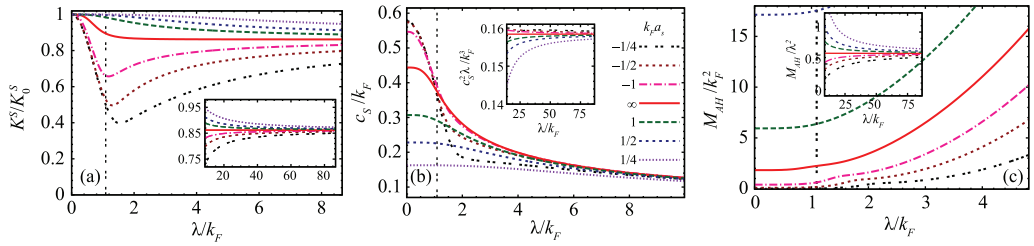

Figure 12: (a) Superfluid phase stiffness (K^S) with $K_0^S = \rho/4$ being the superfluid phase stiffness in free vacuum, (b) Speed of sound (c_S) and (c) Anderson Higgs mass (M_{AH}) as a function of λ for the S gauge field. Large λ limits of these quantities are given in eqn. (48), eqn. (49) and eqn. (50) respectively.

tion) Green's function is defined as

$$G^{-1}_{0\sigma,\sigma'} = \left[ik_n\delta_{\sigma\sigma'} - (\mathcal{H}^R_{\sigma\sigma'}(\boldsymbol{k}) - \mu\delta_{\sigma\sigma'})\right]\delta_{k,k'}, \tag{42}$$

where $k = (ik_n, \boldsymbol{k})$ and $q = (iq_\ell, \boldsymbol{q})$ with $ik_n(iq_l)$ being a Fermi(Bose) Matsubara frequencies. Since the pair operator $S^\star(q) = \sum_{k,\alpha\beta} A_{\alpha\beta}(\boldsymbol{q},\boldsymbol{k}) c^\star_\alpha(\frac{q}{2}+k) c^\star_\beta(\frac{q}{2}-k)$, the effective action can be written in the following way,

$$\mathcal{S}[\phi] = \frac{1}{2}\sum_q \phi^*(q)\left(\kappa(iq_\ell)^2 - q_i K^s_{ij} q_j\right)\phi(q), \tag{43}$$

where $\phi(q)$ is the field corresponding to phase fluctuation and

$$K^s_{ij} = \frac{\Delta^2}{2V}\sum_{\boldsymbol{k}\alpha}\frac{v^\alpha_i(\boldsymbol{k})v^\alpha_j(\boldsymbol{k})}{4E^3_\alpha(\boldsymbol{k})} + \frac{2\Delta^2}{V} \times \sum_{\boldsymbol{k}}\frac{(\varepsilon_+(\boldsymbol{k}) - \varepsilon_-(\boldsymbol{k}))^2}{2E_+(\boldsymbol{k})E_-(\boldsymbol{k})\left(E_+(\boldsymbol{k}) + E_-(\boldsymbol{k})\right)} S_{ij}(\boldsymbol{k}), \tag{44}$$

is the phase stiffness tensor,

$$\kappa = Z + \frac{X^2}{U} \tag{45}$$

is the compressibility. The mass (gap) of the amplitude (Anderson-Higgs) mode is

$$M^2_{AH} = \frac{ZU + X^2}{ZW}. \tag{46}$$

The functions Z, X, U and W at $T = 0$ are given by, $Z = \frac{\Delta^2}{2V}\sum_{\boldsymbol{k}\alpha}\frac{1}{4E^3_\alpha(\boldsymbol{k})}$, $X = \frac{\Delta^2}{2V}\sum_{\boldsymbol{k}\alpha}\frac{\xi_\alpha(\boldsymbol{k})}{2E^3_\alpha(\boldsymbol{k})}$, $U = \frac{\Delta^4}{2V}\sum_{\boldsymbol{k}\alpha}\frac{1}{E^3_\alpha(\boldsymbol{k})}$, $W = \frac{\Delta^2}{2V}\sum_{\boldsymbol{k}\alpha}\frac{\xi^2_\alpha(\boldsymbol{k})}{4E^5_\alpha(\boldsymbol{k})}$, and $E_\alpha(\boldsymbol{k})$ is defined near eqn. (29). In eqn. (44), $v^\alpha_i(\boldsymbol{k}) = \frac{\partial\varepsilon_\alpha(\boldsymbol{k})}{\partial k_i}$, and $S_{ij}(\boldsymbol{k})$ is a tensor defined by $|A_{+-}(\boldsymbol{q},\boldsymbol{k})|^2 = |A_{-+}(\boldsymbol{q},\boldsymbol{k})|^2 \approx q_i S_{ij}(\boldsymbol{k}) q_j$, for small $|\boldsymbol{q}|$. The anisotropic propagation of sound

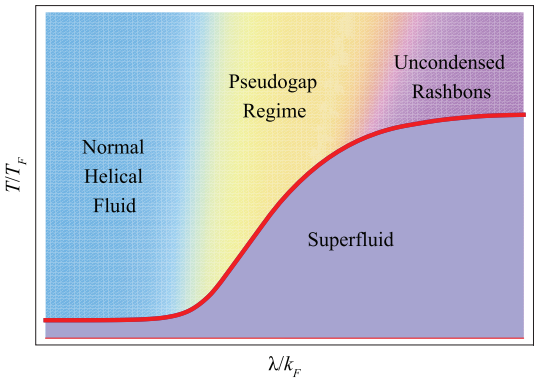

Figure 13: Schematic phase diagram of a system with weak attraction $k_F|a_s| \lesssim 1, a_s < 0$; indicating the nature of the states in various regimes.

is captured by obtaining the speed of sound and in the direction $\hat{\boldsymbol{q}}$ it is given by

$$c^2_s(\hat{\boldsymbol{q}}) = \frac{\hat{q}_i K^s_{ij}\hat{q}_j}{\kappa}. \tag{47}$$

The behaviors of superfluid phase stiffness, speed of sound and the mass of the Anderson Higgs mode are shown as a function of λ for the spherical GFC in fig. 12(a), fig. 12(b) and fig. 12(c) respectively. We see that the superfluid density is not same as the particle density and has a characteristic non-monotonic behavior. This owes to the absence of Galilean invariance in presence of the gauge field. The non-zero value of the superfluid stiffness seen in fig. 12(a) and that of sound speed seen in fig. 12(b) suggest that there is interaction amongst the rashbons.

We now consider the most interesting regime where the ground state is a RBEC. In this regime $\lambda \gg k_F, \frac{1}{a_s}$ and it is found that the phase stiffness is determined by the rashbon mass. For the spherical gauge field K^s is isotropic

$$K^s = \frac{\rho_R}{m_R}, \tag{48}$$

where $\rho_R = \rho/2$ is density of the rashbons with mass m_R, speed of sound is

$$c_s^2 = \frac{2\pi\rho}{m_R}\left(\frac{\sqrt{3}}{\lambda}\right), \tag{49}$$

and the mass of the Anderson-Higgs mode is

$$M_{AH} = \frac{2}{3}\lambda^2. \tag{50}$$

The behavior of K^s in this limit is in accordance with Legget's theorem and implies reemergence of Galilean invariance. Comparing the expressions of the speed of sound and the mass with those obtained in the standard Bogoliubov theory of anisotropic bosons[40] yields the effective rashbon-rashbon scattering length. For example, for spherical gauge field, the rashbon-rashbon scattering length is,

$$a_R = \frac{m^R\sqrt{3}}{\lambda} = \frac{3\sqrt{3}(4+\sqrt{2})}{7}\frac{1}{\lambda} \approx \frac{4}{\lambda}. \tag{51}$$

This is found to be solely dependent upon λ. This suggests that the effective interaction between the rashbons depends only on the gauge field and not on the interaction between their constituent fermions!

The estimation of transition temperature discussed earlier is based on mean field theory and two body analysis. The Gaussian fluctuation above the mean field ground state also gives an estimate of transition temperature which will be discussed in a forthcoming paper[41] alongwith some more interesting physics. The normal state above the transition temperature also has some interesting features (fig. 13) which are important from the experimental point view.

6 Experimental Relevance

In this section we discuss the experimental relevance of the physics discussed in this article. Several encouraging experimental efforts have been made with spin-orbit coupled bosons.[8–12] Recently, in experiments[13,14] with fermionic systems with synthetic gauge fields, a close cousin of the EP gauge field called the SM gauge fields have been realized. This gauge field is, in fact, the EP gauge field with two additional magnetic fields. Unfortunately, it does not produce a rashbon condensate but there are many other interesting phenomena that occur in the presence of this gauge field.[42] The Rashba gauge field is yet to be realized because of the key difficulty associated with the heating caused by the spontaneous emission due to the interaction of the atoms with the lasers. There is a very interesting proposal using a pulsed magnetic field on an atom chip to produce the spin orbit coupling of the Rashba type[19,20] which would overcome this difficulty. If the physics discussed here is realized in real materials, it could lead to the development of materials with high transition temperatures, even to room temperatures!

7 Conclusion and Future Directions

In this review, we have considered the physics of two-component Fermi gas in the presence of $SU(2)$ synthetic non-Abelian gauge fields which induce a generalized Rashba type spin-orbit coupling. The key points of this article can be summarized as follows:

1. There is a change in the topology of the non-interacting Fermi surface with changing the strength of the non-Abelian gauge field. In particular, the positive helicity Fermi surface vanishes after a critical gauge field strength λ_T.
2. The non-interacting Fermi gas in the presence of an isotropic trapping potential and synthetic non-Abelian gauge fields has the potential to produce novel Hamiltonians and lead to characteristic change in the density profile of the cloud.
3. For zero center of mass momentum, the non-Abelian gauge fields always help in the formation of two-body bound states and hence act as an attractive interaction amplifier. Special classes of gauge fields admit formation of bound states for arbitrary weak attraction even in three spatial dimension! The bound state wave-functions have interesting spin structures.
4. After a critical value of center of mass momentum, the two-body bound state vanishes due to the lack of Galilean invariance.
5. Even with a fixed weak attraction the many body system undergoes a BCS to BEC crossover only by tuning the gauge field strength.
6. At large gauge coupling strength, the BEC obtained is a condensate of new kind of bosons, called *rashbons*. The properties of these new kind of emergent particles, including their interaction strength, depend only on the gauge field strength and not on their constituent particles!
7. Being in the BCS side of the crossover, when the gauge field strength is tuned to obtain RBEC, in this process the transition temperature is increased from exponentially small value to the order of the Fermi temperature!

8. The study of the collective excitations over the superfluid ground states indicate that although the system explicitly breaks Galilean invariance, there is an emergent Galilean invariance for large gauge coupling strength.

The synthetic non-Abelian gauge fields have interesting consequences on the Feshbach resonances as well as flows of a superfluid.[43,44] Finally, the problem of fermions in the presence of synthetic gauge fields has many important future prospects. Non trivial topological features of the Fermi surface is expected in the presence of SU(M) gauge fields and this may lead to new kind of FSTT with the possibility of formation of topological superfluid and rashbon like states. Understanding and realizing these physics in real materials may lead to the production of the golden egg of room temperature superconductors.

Acknowledgement

SKG acknowledges support from CSIR, India via SRF grant. The authors acknowledge Vijay B. Shenoy for extensive discussions.

Received 29 May 2014.

References

1. W. D. Phillips, Rev. Mod. Phys. **70**, 721 (1998).
2. S. Chu, Rev. Mod. Phys. **70**, 685 (1998).
3. C. N. Cohen-Tannoudji, Rev. Mod. Phys. **70**, 707 (1998).
4. M. H. Anderson, J. R. Ensher, M. R. Matthews, C. E. Wieman, and E. A. Cornell, Science **269**, 198 (1995).
5. R. Feynman, International Journal of Theoretical Physics **21**, 467 (1982).
6. N. R. Cooper, Advances in Physics **57**, 539 (2008).
7. J. Dalibard, F. Gerbier, G. Juzeliūnas, and P. Öhberg, Rev. Mod. Phys. **83**, 1523 (2011).
8. Y.-J. Lin, R. L. Compton, K. Jimenez-Garcia, J. V. Porto, and I. B. Spielman, Nature **462**, 628 (2009).
9. Y.-J. Lin, R. L. Compton, A. R. Perry, W. D. Phillips, J. V. Porto, and I. B. Spielman, Phys. Rev. Lett. **102**, 130401 (2009).
10. Y.-J. Lin, K. Jimenez-Garcia, and I. B. Spielman, Nature **471**, 83 (2011).
11. R. A. Williams, L. J. LeBlanc, K. Jimenez-Garcia, M. C. Beeler, A. R. Perry, W. D. Phillips, and I. B. Spielman, Science **335**, 314 (2012).
12. J.-Y. Zhang, S.-C. Ji, L. Zhang, Z.-D. Du, W. Zheng, Y.-J. Deng, H. Zhai, S. Chen, and J.-W. Pan, ArXiv e-prints (2013), arXiv:1305.7054.
13. P. Wang, Z.-Q. Yu, Z. Fu, J. Miao, L. Huang, S. Chai, H. Zhai, and J. Zhang, Phys. Rev. Lett. **109**, 095301 (2012).
14. L. W. Cheuk, A. T. Sommer, Z. Hadzibabic, T. Yefsah, W. S. Bakr, and M. W. Zwierlein, Phys. Rev. Lett. **109**, 095302 (2012).
15. D. Jaksch and P. Zoller, New J. Phys. **5**, 56 (2003).
16. K. Osterloh, M. Baig, L. Santos, P. Zoller, and M. Lewenstein, Phys. Rev. Lett. **95**, 010403 (2005).
17. J. Ruseckas, G. Juzeliūnas, P. Öhberg, and M. Fleischhauer, Phys. Rev. Lett. **95**, 010404 (2005).
18. F. Gerbier and J. Dalibard, New J. Phys. **12**, 033007 (2010).
19. Z.-F. Xu, L. You, and M. Ueda, Phys. Rev. A **87**, 063634 (2013).
20. B. M. Anderson, I. B. Spielman, and G. Juzeliūnas, Phys. Rev. Lett. **111**, 125301 (2013).
21. T. D. Stanescu, B. Anderson, and V. Galitski, Phys. Rev. A **78**, 023616 (2008).
22. T.-L. Ho and S. Zhang, Phys. Rev. Lett. **107**, 150403 (2011).
23. C. Wang, C. Gao, C.-M. Jian, and H. Zhai, Phys. Rev. Lett. **105**, 160403 (2010).
24. W. Cong-Jun, I. Mondragon-Shem, and Z. Xiang-Fa, Chinese Physics Letters **28**, 097102 (2011).
25. R. Sachdeva and S. Ghosh, Phys. Rev. A **85**, 013642 (2012).
26. J. P. Vyasanakere and V. B. Shenoy, Phys. Rev. B **83**, 094515 (2011).
27. J. P. Vyasanakere, S. Zhang, and V. B. Shenoy, Phys. Rev. B **84**, 014512 (2011).
28. J. P. Vyasanakere and V. B. Shenoy, New J. Phys. **14**, 043041 (2012).
29. S. K. Ghosh, J. P. Vyasanakere, and V. B. Shenoy, Phys. Rev. A **84**, 053629 (2011).
30. J. P. Vyasanakere and V. B. Shenoy, Phys. Rev. A **86**, 053617 (2012).
31. R. Winkler, *Spin Orbit Coupling Ects in Two-Dimensional Electron and Hole Systems* (Springer, Berlin, 2003).
32. J. K. Jain, *Composite Fermions* (Cambridge University Press, Cambridge, UK, 2007).
33. C. J. Pethick and H. Smith, *Bose-Einstein Condensation in Dilute Gases* (Cambridge University Press, 2004).
34. E. Braaten, M. Kusunoki, and D. Zhang, Ann. Phys. **323**, 1770 (2008).
35. J. R. Taylor, *Scattering Theory* (Dover Publications, New York, 2006).
36. A. J. Leggett, *Quantum Liquids: Bose Condensation and Cooper Pairing in Condensed-Matter Systems* (Oxford University Press, 2006).
37. M. Sigrist and K. Ueda, Rev. Mod. Phys. **63**, 239 (1991).
38. M. Randeria, in *Bose-Einstein Condensation*, edited by A. Griffin, D. Snoke, and S. Stringari (Cambridge University Press, 1995) Chap. 15.
39. Z.-Q. Yu and H. Zhai, Phys. Rev. Lett. **107**, 195305 (2011).
40. A. A. Abrikosov, L. P. Gor'kov, and I. Y. Dzyaloshinskii, *Quantum field theoretical methods in statistical physics* (Pergamon, 1965).
41. J. P. Vyasanakere and V. B. Shenoy, Manuscript under preparation.
42. V. B. Shenoy and J. P. Vyasanakere, J. Phys. B: At. Mol. Opt. Phys. **46**, 134009 (2013).
43. V. B. Shenoy, Phys. Rev. A **88**, 033609 (2013).
44. V. B. Shenoy, Phys. Rev. A **89**, 043618 (2014).

Sambuddha Sanyal obtained his B.Sc. with Physics honours from the University of Calcutta, Kolkata in 2006. After that he joined Indian Institute of Technology, Delhi, where he worked on hot and dense hadronic matter under the guidance of Amruta Mishra, and obtained his masters degree in 2008. Followed by that he did his Ph.D. at Tata Institute of Fundamental Research, Mumbai, under the guidance of Kedar Damle. His dissertation was on disorders in strongly correlated systems. Presently, he is a research associate at the centre of Condensed matter theory of Indian Institute of Science, Bangalore. His current research interests are in the areas of strongly correlated systems and ultra cold atoms.

Sudeep Kumar Ghosh obtained his undergraduate degree in Physics from Jadavpur University, Kolkata in 2009. He then moved to Indian Institute of Science, Bangalore under the Integrated Ph.D. program to pursue full time Ph.D. under the supervision of Vijay B. Shenoy in the same year. Currently, he is working on the system of ultra cold atoms in synthetic gauge fields.

Jayantha Vyasanakere obtained his undergraduate degree from Bangalore University in 2008. He then joined Indian Institute of Science, Bangalore to pursue integrated MS and Ph.D. program. Recently, he completed his Ph.D. on Ultracold fermions in synthetic non-Abelian gauge fields under the supervision of Vijay B. Shenoy. Currently he is working as an Assistant Professor of Physics at Tumkur University, Tumkur.